Hindawi
Complexity
Volume 2019, Article ID 6469853, 11 pages
https://doi.org/10.1155/2019/6469853

Research Article

Assessment of Diabetic Autonomic Nervous Dysfunction with a Novel Percussion Entropy Approach

Hai-Cheng Wei,[1] Ming-Xia Xiao,[1,2] Na Ta,[1] Hsien-Tsai Wu,[3] and Cheuk-Kwan Sun [4]

[1]*School of Electrical and Information Engineering, North Minzu University, No. 204 North – Wenchang St., Xixia District, Yinchuan, Ningxia 750021, China*
[2]*School of Computer and Information, Hefei University of Technology, No. 193, Tunxi Rd., Hefei, Anhui 230009, China*
[3]*Department of Electrical Engineering, National Dong Hwa University, No. 1, Sec. 2, Da Hsueh Rd., Shoufeng, Hualien 97401, Taiwan*
[4]*Department of Emergency Medicine, E-Da Hospital, I-Shou University School of Medicine for International Students, No. 1, Yida Road, Jiaosu Village, Yanchao District, Kaohsiung City 82445, Taiwan*

Correspondence should be addressed to Cheuk-Kwan Sun; lawrence.c.k.sun@gmail.com

Received 19 June 2018; Revised 21 October 2018; Accepted 28 January 2019; Published 19 February 2019

Guest Editor: Gábor Szederkényi

This study investigated the validity of a novel parameter, percussion entropy index (PEI), for assessing baroreflex sensitivity. PEI was acquired through comparing the similarity in tendency of change between the amplitudes of successive digital volume pulse (DVP) signals and changes in R-R intervals (RRI) of successive cardiac cycles. Totally 108 upper middle-aged volunteers were divided into three groups: healthy subjects (Group 1, age 41–80, n=41), those with well-controlled type 2 diabetes mellitus (T2DM) (Group 2, age 41–82, n=36, glycated hemoglobin (HbA1c)<6.5%), and patients with poorly controlled T2DM (Group 3, age 44–77, n=31, HbA1c≧6.5%). Percussion entropy index (PEI) was computed from DVP signals acquired through photoplethysmography (PPG) and RRI from electrocardiogram in 1000 successive cardiac cycles for each subject. Autonomic function was also assessed by Poincaré index (SD1/SD2 ratio, SSR), low- to high-frequency power ratio (LFP/HFP, LHR), and small-scale multiscale entropy index (MEI_{SS}) for comparison. Demographic, anthropometric, hemodynamic, and serum biochemical parameters of all testing subjects were obtained for investigating the significance of associations with the three parameters. The results showed that MEI_{SS} and PEI successfully discriminated among the three groups ($p<0.017$). However, only PEI showed significant associations with indicators of both acute (i.e., fasting blood sugar concentration, $p<0.017$) and chronic (i.e., HbA1c level, $p<0.001$) blood sugar control. Multivariate analysis also showed significant associations of PEI with fasting blood sugar and HbA1c levels in all subjects. The interpreting effect of the two independent variables, HbA1c level and fasting blood sugar concentration, on PEI was 71.4% and 12.3%, respectively. In conclusion, the results demonstrated that additional information on diabetic autonomic dysfunction can be obtained through comparing two simultaneously acquired physiological time series. The significant associations of percussion entropy index with indicators of blood sugar control also highlight its possible role in early screening of the disease.

1. Introduction

Diabetes mellitus (DM) is a dominant metabolic disease worldwide with an estimated prevalence of 108 million in 1980, which soared by almost four times to 422 million in 2014 and is still on the increase [1]. Patients with type 2 DM are at increased risk of developing autonomic nervous dysfunction [2], atherosclerosis [3, 4], and even cancers [5]. Therefore, early diagnosis and treatment are of vital importance. Clinically, retinopathy [6], nephropathy [7], and neuropathy [8] are the three hallmarks of the disease [9]. Although the former two can be diagnosed through physical examination and laboratory study, respectively, the latter cannot be easily assessed objectively. The adverse impact of diabetes-associated neurological damage cannot be overemphasized. In addition to diabetic sensory and motor neuropathy [8], a number of studies have shown significant associations between compromised autonomic nervous function and an increased risk of cardiovascular morbidity and mortality [10–12]. Besides, depressed autonomic function has been found to be a predictor of rapid progression of atherosclerosis [13].

Baroreflex is a physiological phenomenon in which an increase in blood pressure would lead to a prolongation of the R-R interval (RRI). Accordingly, a decrease in blood pressure would shorten the RRI [14]. It is a physiological compensatory mechanism to maintain hemodynamic stability of an individual [15]. Baroreflex sensitivity, which refers quantitatively to the degree of matching between a change in blood pressure and a change in interbeat intervals (i.e., RRI) of the heart [14, 16], has been found to be impaired in patients with systemic diseases such as diabetes [2, 11, 17]. Previous studies have demonstrated the successful application of noninvasive approaches to assessing autonomic function. For instance, frequency domain analysis of heart rate variability (HRV) based on R-R intervals (RRI) from electrocardiograph (EKG) is an assessment method for autonomic nervous activity and baroreflex sensitivity [14]. The parameter of low- to high-frequency power ratio (LFP/HFP, LHR) thus obtained is considered to reflect the relative activities of the sympathetic and parasympathetic nervous systems [17–19]. However, such a frequency domain parameter has its limitations because of the nonstationary and nonlinear nature of the physiological signals to be analyzed [20–22]. In an attempt to tackle this problem, the Poincaré index (SD1/SD2 ratio, SSR) was introduced to assess autonomic nervous activities and baroreflex sensitivity using a nonlinear approach to analyzing HRV [20, 23]. Nevertheless, both frequency (i.e., LHR) and time (i.e., SSR) domain analyses assess autonomic activities (i.e., HRV) merely based on a one-dimensional time series (i.e., RRI) without taking into account other simultaneous physiological changes.

Multiscale entropy (MSE), which was first proposed by Costa et al. [24], is a method for analyzing the complexity of nonlinear and nonstationary signals in finite length time series. It was used to analyze the complexity of a single time series (i.e., RRI) to differentiate between healthy and diseased subjects [24]. The present study attempted to apply a novel parameter of "percussion entropy index (PEI)" to assess baroreflex sensitivity by comparing the degree of matching between the changes of two autonomic function-related time series (i.e., amplitude of digital volume pulse and RRI) during successive cardiac cycles to more accurately investigate an individual's autonomic functions. The concept of percussion entropy index (PEI) in the present study is based on that of MSE index (MEI). The difference between small-scale multiscale entropy index (MEI_{SS}) and PEI is that the former evaluates the degree of fluctuations of a parameter within a defined region in a time series, whereas the latter is a simple means to assess the similarity in the pattern of changes (i.e., increase or decrease) of two related time series to evaluate the adaptive capacity of a physiological system.

Although baroreflex sensitivity (BRS) has been shown to be a good indicator of autonomic activity [15], assessment of BRS requires the simultaneous acquisition of information on real-time blood pressure and HRV. Previous studies have demonstrated that the sensitivity of BRS assessment by noninvasive means is comparable to that acquired through invasive measurement [14, 25]. Digital volume pulse (DVP) signals acquired noninvasively through photoplethysmography (PPG) have been found to correlate well with changes in blood pressure [26–28]. Besides, the current study was designed based on the finding that baroreceptor sensitivity was impaired in subjects with chronic systemic diseases, particularly those that affect the cardiovascular system (e.g., diabetes) [2, 11, 17]. Using percussion entropy index (PEI), the present study is aimed at investigating the validity of a two-dimensional approach to the assessment of diabetes-associated changes in autonomic activities using two noninvasively acquired time series, including waveform amplitudes of DVP signals from finger and RRI. Results of autonomic function assessment from data on RRI using time (i.e., Poincaré index: SD1/SD2 ratio, SSR) and frequency (i.e., low- to high-frequency power ratio: LFP/HFP, LHR) domain analyses as well as MEI_{SS} were also obtained for comparison.

The rest of this paper is organized as follows: Section 2 comprises study population (i.e., study period, criteria for subject recruitment, and grouping), study protocol (i.e., comparison of the computational parameters with the demographic, anthropometric, hemodynamic, and serum biochemical parameters of the three groups of testing subjects), details on data acquisition and analysis including calculation of unilateral fingertip PPG amplitude sequence and RRI sequence (i.e., Amp and RRI), and computation of multiscale small-scale entropy index (MEI_{SS}) and percussion entropy index (PEI) as well as statistical analysis. In Section 3, the choice of shift number for percussion entropy index computation was first justified, followed by the comparison of the four computational parameters for autonomic function assessment. In Sections 4 and 5, discussion and conclusions derived from this study are summarized with several suggestions for future work.

2. Methods

2.1. Study Population. Between July 2009 and Feb. 2012, 114 volunteers were recruited for the present study. All diabetic patients were enrolled from the diabetes outpatient clinic of the Hualien Hospital, while healthy controls were recruited from a physical check-up program at the same hospital. Of the 114 volunteers, 6 were excluded due to incomplete or unstable waveform data acquisition. The remaining 108 subjects were then divided into three groups, namely, healthy upper middle-aged subjects (Group 1, age range: 41-80, number = 41), upper middle-aged subjects diagnosed as having type 2 DM with satisfactory blood sugar control (Group 2, age range: 41-82, number = 36, glycated hemoglobin (HbA1c) < 6.5%), and type 2 diabetic patients with poor blood sugar control (Group 3, age range: 44-77, number = 31, HbA1c $\geqq$ 6.5%) (Table 1). All healthy subjects had no personal or family history of cardiovascular diseases. Type 2 diabetes was diagnosed by either a fasting blood sugar concentration $\geqq$ 126 mg/dL or HbA1c $\geqq$ 6.5% [29]. All diabetic patients underwent regular treatment and follow-up in outpatient clinic for at least two years. Each subject was required to refrain from theophylline-containing medications and caffeine-containing beverages for at least 8 hours before acquisition of data. Before taking the tests, all subjects were requested to sign informed consent and complete questionnaires on demographics and medical histories as well as

Table 1: Demographic, anthropometric, hemodynamic, and serum biochemical parameters of the testing subjects.

Parameters	Group 1 (number: 41)	Group 2 (number: 36)	Group 3 (number: 31)
Female/male	24/17	16/20	11/20
Age (year)	56.75 ± 3.88	59.16 ± 8.40	56.08 ± 11.38
Body height (cm)	163.49 ± 8.30	162.59 ± 7.95	163.39 ± 5.20
Body weight (kg)	65.01 ± 13.78	71.59 ± 11.89	79.69 ± 16.35
WC (cm)	81.74 ± 11.81	94.25 ± 9.72**	100.69 ± 13.51†
BMI (kg/m^2)	24.17 ± 4.12	26.96 ± 2.87*	29.87 ± 6.05
SBP (mmHg)	116.41 ± 15.63	125.71 ± 18.06	126.69 ± 10.29
DBP (mmHg)	73.70 ± 9.70	74.06 ± 12.41	76.38 ± 4.23
PP (mmHg)	42.41 ± 10.73	51.65 ± 11.94	50.31 ± 12.07
HDL (mg/dL)	53.22 ± 20.81	44.07 ± 9.89	40.50 ± 9.68
LDL (mg/dL)	122.34 ± 29.49	94.36 ± 21.93	118.10 ± 29.91
Cholesterol (mg/dL)	192.46 ± 40.01	170.80 ± 31.00	199.09 ± 34.63†
Triglyceride (mg/dL)	98.05 ± 85.35	112.93 ± 39.92	185.91 ± 74.89†
HbA1c (%)	5.68 ± 0.38	6.95 ± 0.39**	9.25 ± 1.63††
Fasting blood sugar (mg/dL)	93.98 ± 10.67	127.47 ± 25.70**	176.91 ± 68.71†

Group 1: healthy subjects; Group 2: diabetic subjects with satisfactory blood sugar control; Group 3: diabetic subjects with poor blood sugar control. Values are expressed as mean ± SD; WC: waist circumference; BMI: body mass index; SBP: systolic blood pressure; DBP: diastolic blood pressure; PP: pulse pressure; HbA1c: glycated hemoglobin. *$p < 0.017$: Group 1 vs. Group 2; **$p < 0.001$: Group 1 vs. Group 2; †$p < 0.017$: Group 2 vs. Group 3, and ††$p < 0.001$: Group 2 vs. Group 3.

receive blood sampling for serum biochemical analysis. The study was approved by the Institutional Review Board (IRB) of Hualien Hospital.

2.2. Study Protocol. One waveform parameter (i.e., amplitude, Amp) and one parameter of cardiac electricalactivity (i.e., RRI) were acquired from all subjects. Autonomic function analysis was performed on the acquired data of RRI from the frequency [17–19] and time [20, 23] domains to obtain the low- to high-frequency power ratio (LFP/HFP, LHR) and Poincaré index (SD1/SD2 ratio, SSR), respectively. Percussion entropy index (PEI) was computed from the synchronized Amp and RRI time series for each testing subject. The associations of the computational parameters thus obtained (i.e., PEI, MEI_{SS}, LHR, SSR) with the demographic (i.e., age), anthropometric (i.e., body height, body weight, waist circumference, body-mass index), hemodynamic (i.e., systolic and diastolic blood pressures), and serum biochemical (i.e., high- and low-density lipoprotein cholesterol, total cholesterol, and triglyceride) parameters of the three groups of testing subjects were then analyzed and compared.

2.3. Data Acquisition and Analysis. All participants were required to rest supinely in a quiet, temperature-controlled room at 25 ± 1°C for 4 minutes before 30 minutes of measurement. Using an automated oscillometric device (BP3AG1, Microlife, Taiwan) with an inflatable cuff of appropriate size, blood pressure was obtained once over left arm in supine position. Data on left index finger waveform were collected with a six-channel EKG-photoplethysmography (PPG) system as described previously [30, 31]. The digitized signals (both PPG and ECG) were processed through an analog-to-digital converter (USB-6009 DAQ, National Instruments, Austin, TX) using a sampling frequency of 500 Hz before being stored in a computer for later analysis. The digital volume pulses (DVPs) were acquired through PPG as previously reported [30]. In the present study, DVPs from the fingertip were used for waveform contour analysis. The systolic peak and foot point were identified from the contour of the DVP. The amplitude of each waveform (Amp) was defined as that between the foot point and the systolic peak of a pulse wave [32] (Figure 1).

2.3.1. Calculation of Unilateral Fingertip PPG Amplitude Sequence and RRI Sequence (i.e., Amp and RRI). Time series of DVP waveform amplitude, $\{\mathrm{Amp}(j)\} = \{\mathrm{Amp}(1), \mathrm{Amp}(2), \ldots, \mathrm{Amp}(n)\}$, and that of RRI, $\{\mathrm{RRI}(i)\} = \{\mathrm{RRI}(1), \mathrm{RRI}(2), \ldots, \mathrm{RRI}(n)\}$, were simultaneously acquired from n successive and stable cardiac cycles with photoplethysmography (PPG) and EKG, respectively, for each testing subject [33]:

$$\{\mathrm{Amp}\} = \{\mathrm{Amp}(1), \mathrm{Amp}(2), \mathrm{Amp}(3), \ldots, \mathrm{Amp}(n)\} \quad (1)$$

$$\{\mathrm{RRI}\} = \{\mathrm{RRI}(1), \mathrm{RRI}(2), \mathrm{RRI}(3), \ldots, \mathrm{RRI}(n)\}. \quad (2)$$

2.3.2. Computation of Multiscale Small-Scale Entropy Index (MEI_{SS}). Multiscale entropy (MSE) was first proposed by Costa et al. [21] as a method for analyzing the complexity of time series of nonlinear signals in 2002 using the RRI time series as mentioned in (2) above. MSE consists of two main procedures, including coarse-graining and computation of sample entropy for each coarse-grained time series as detailed below.

(1) Coarse-Graining. Coarse-graining is the process of creating new time series of different lengths through averaging

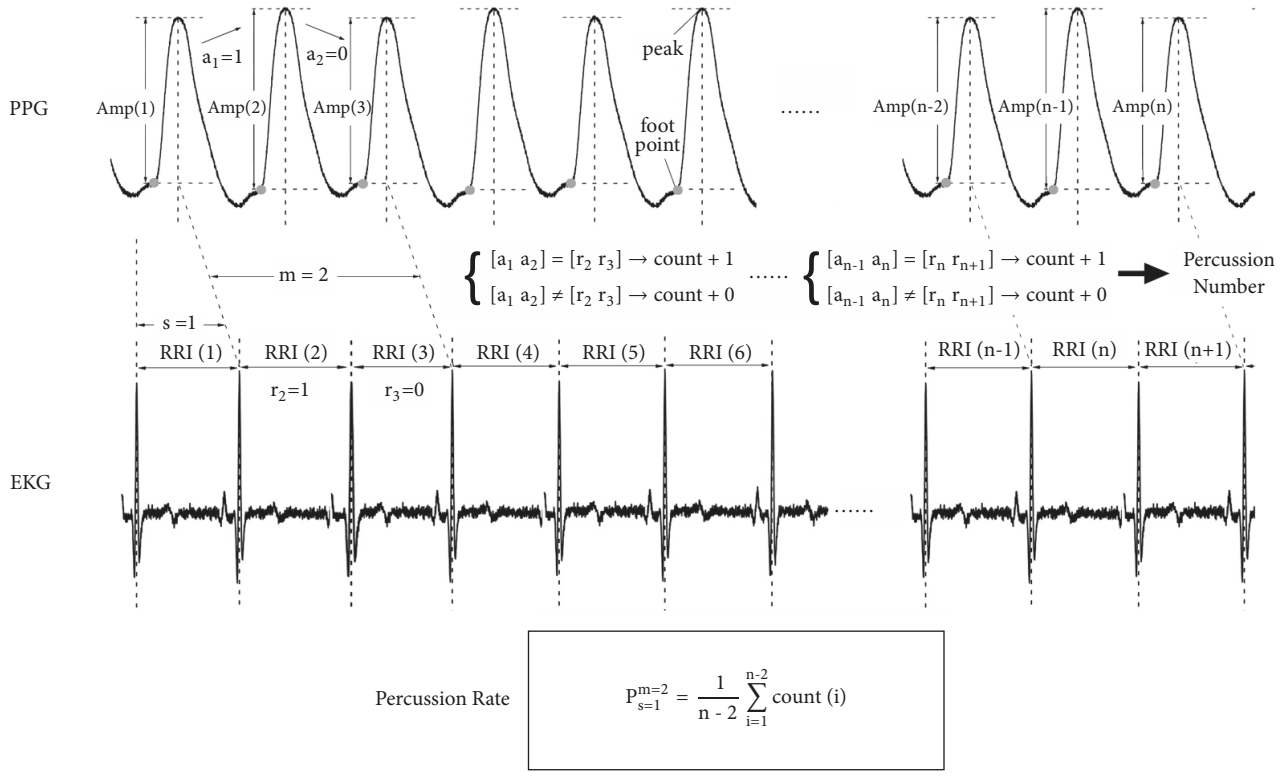

Figure 1: Computation of percussion rate by matching changes in the amplitudes (Amp, defined as the height of a waveform from foot point to peak) of n successive photoplethysmography (PPG)-acquired digital volume pulse (DVP) waveforms with changes in R-R intervals (RRI) using a shift number (s) of 1 and the dimension of vector pattern (m) (i.e., impact points) of 2. Note that n = 1000 for the present study. PPG: photoplethysmography; EKG: electrocardiogram; Amp(n): amplitude of DVP waveform during n^{th} cardiac cycle; RRI(n): R-R interval during n^{th} cardiac cycle; a: binary code denoting increase (i.e., 1) or decrease (i.e., 0) in amplitude when compared with the previous waveform; r: binary code denoting increase (i.e., 1) or decrease (i.e., 0) in RRI when compared with the previous cardiac cycle.

successive points in the original series according to a scale factor, τ, which is the number of points to be included:

$$\text{RRI}(a)^{\tau} = \frac{1}{\tau}\sum_{i=(a-1)\tau+1}^{a\tau} \text{RRI}(i), \quad 1 \le a \le \frac{n}{\tau},\ a \text{ is positive integer number.} \tag{3}$$

Here n is the number of points in the original {RRI} time series (i.e., n = 1000 in the present study). RRI(i) refers to the duration of RRI of the i^{th} cardiac cycle (2). RRI$(a)^{\tau}$ is the value of RRI during the a^{th} cardiac cycle in the new time series created according to τ ($\tau = 1, 2, \ldots, 10$ in the present study).

For instance, coarse-graining (i.e., (3)) can transform a time series {RRI} with 1000 points to a new series with 500 points when $\tau = 2$ and to another time series with 333 points when $\tau = 3$. Following the same pattern of computation, a time series with 100 points can be obtained when $\tau = 10$. In other words, through coarse-graining, the original {RRI} time series can be transformed into 10 series of different lengths (i.e., number of points). For the purpose of the present study, the sample entropy for each of the 10 series was computed for analysis.

(2) Sample Entropy. Sample entropy was first introduced in the year 2000 for the assessment of complexity in physiological time series [34]. The computation of sample entropy involves three parameters, namely, m, r, and n. While m is the dimension of vector pattern (i.e., impact points), r is the range of acceptable fluctuation within the comparable time segments and n is the number of points in the time series (i.e., length of the series). The process of computation is described as follows:

(1) R-R intervals (RRI) of different time scales were grouped into n-m+1 vectors with dimension m:

$$u_m(i) = [\text{RRI}(j)\ \ \text{RRI}(j+1)\ \ \text{RRI}(j+2)\ \cdots\ \text{RRI}(j+m-1)], \quad 1 \le j \le n-m+1. \tag{4}$$

For instance, to analyze the changes in RRI among three cardiac cycles, m is set at 2 (Figure 1). Accordingly, to discern the fluctuations among four cardiac cycles, m is set at 3. For the purpose of the present study that analyzed 1000 cardiac cycles, m was set at 2 and 3 for the assessment of complexity of signals acquired from each testing subject.

(2) Define $d[u_m(i), u_m(j)]$ as the maximum value:

$$d\left[u_m(i), u_m(j)\right] = \max\left\{\left|RRI(i+k) - RRI(j+k)\right| : 0 \le k \le m-1\right\}, \quad (i \ne j). \tag{5}$$

Two time segments were considered comparable when the absolute value of the difference between their respective components was less than the range of acceptable fluctuation, r (i.e., $d[u_m(i), u_m(j)] \le r$ in (5)). The acceptable range, r, was defined as $0.15 \times$ SD (where SD is the standard deviation of the original time series) according to a previous study [35].

(3) Count the number of $d[u_m(i), u_m(j)]$ within r distance, and let $no_m(r)$ represent the number of vectors $u_m(j)$ within r distance of $u_m(i)$. Therefore, $C^m(r)$ in (6) represents the probability that any vectors $u_m(j)$ exist within r distance of $u_m(i)$.

$$C^m(r) = \frac{no_m(r)}{(n-m+1)} \tag{6}$$

(4) The mean of the probability of similarity of n-m+1 sets of data is denoted by $\Phi^m(r)$.

$$\Phi^m(r) = \frac{1}{n-m+1}\sum_{j=1}^{N-m+1} C^m(r) \tag{7}$$

(5) Similarly, repeating step (1) to step (4) above with m+1 gives $\Phi^{m+1}(r)$. The sample entropy of the RRI time series at a particular time scale can then be obtained.

$$\text{Sample entropy}\left(S_E\right) = \ln\left(\Phi^m(r)\right) - \ln\left(\Phi^{m+1}(r)\right) = \ln\frac{\Phi^m(r)}{\Phi^{m+1}(r)} \tag{8}$$

After acquisition of 10 time series from (3) using different time scales (i.e., τ from 1 to 10), the corresponding sample entropy for each time series was computed using (8). Each sample entropy value provides information on an aspect of complexity. Previous studies have reported that small-scale entropy index (MEI_{SS}) and large-scale entropy index (MEI_{LS}) obtained by taking the average of sample entropy values from 1 to 5 and from 6 to 10, respectively, can reflect the complexity of different physiological systems. While MEI_{SS} represents the complexity of signals from the autonomic nervous system, MEI_{LS} reflects signal complexity of the vascular system [35, 36]. Accordingly, since the present study is aimed at investigating autonomic nervous function, MEI_{SS} of the testing subjects was acquired for comparison.

$$MEI_{SS} = \frac{1}{5}\sum_{\tau=1}^{5}\left(S_E\right) \tag{9}$$

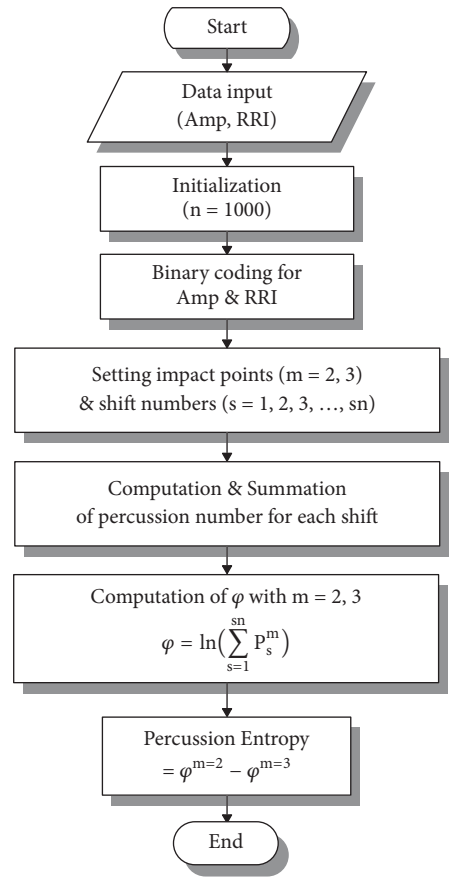

Figure 2: Flow chart of percussion entropy computation. Amp: amplitude; RRI: R-R interval.

2.3.3. Computation of Percussion Entropy Index (PEI). The computation of percussion entropy index (PEI) comprises the following (Figure 2).

Step 1. Binary sequence transformation for {Amp} and {RRI}

$$B_{Amp} = \{a_1\ a_2\ a_3\ \cdots\ a_n\}, \quad a_i = \begin{cases} 0, & Amp(i+1) \le Amp(i) \\ 1, & Amp(i+1) > Amp(i) \end{cases} \tag{10}$$

$$B_{RRI} = \{r_1\ r_2\ r_3\ \cdots\ r_n\}, \quad r_i = \begin{cases} 0, & RRI(i+1) \le RRI(i) \\ 1, & RRI(i+1) > RRI(i) \end{cases} \tag{11}$$

Based on the previous finding that the change in amplitudes of DVP waveforms reflects the fluctuation in blood pressure [26–28] that gives rise to a corresponding compensatory change in RRI because of baroreflex, the fluctuations among successive DVP waveform amplitudes and RRIs undergo binary transformation to give two binary sequences (i.e., B_{Amp} and B_{RRI}, respectively).

Step 2. Define the series B_{Amp} and B_{RRI} with length n as well as the two parameters of m and sn [where m is the impact points (i.e., embedded dimension of vectors); sn is the shift number of B_{RRI}].

Step 3. Define n – m + 1 vectors of sample pattern, each of size m, composed as follows:

$$B_{Amp}(i) = \{a_i, a_{i+1}, \ldots, a_{i+m-1}\}, \quad 1 \le i \le n-m+1. \tag{12}$$

Step 4. For s = 1 to sn (i.e., shift numbers) for the series B_{RRI}

$$B_{RRI}(i+s) = \{r_{i+s}, r_{i+s+1}, \ldots, r_{i+s+m-1}\}, \quad 1 \le i \le n-m+1, \ s = 1 \text{ to sn}. \tag{13}$$

Although an increase in blood pressure would cause a prolongation of RRI in the next cardiac cycle in healthy young subjects, this baroreflex response may be delayed in the elderly or those with systemic diseases [2, 11, 17]. Therefore, we assumed that variations in baroreflex sensitivity would cause corresponding delays (counted as number of cardiac cycles, i.e., 1, 2, 3... sn) in the effects of blood pressure changes (i.e., reflected in DVP amplitudes) on RRI.

Step 5. Count the match number for $B_{Amp}(i)$ and $B_{RRI}(i + s)$ with given m.

In addition, calculate the total match number of $B_{Amp}(i)$ and $B_{RRI}(i+s)$ with the same pattern (i.e., percussion number) and divide by the total number of vectors of pattern (n-m-s+1) to obtain the percussion rate, which is defined as

$$P_s^m = \frac{1}{(n-m-s+1)} \sum_{i=1}^{n-m-s+1} \text{count}(i). \tag{14}$$

For example (Figure 1), $P_{s=1}^{m=2} = (1/(n-2)) \sum_{i=1}^{n-2} \text{count}(i)$ is a binary amplitude series (B_{Amp}) to be compared to a binary RRI series (B_{RRI}) with a left shift of one cardiac cycle (s=1) in the same testing subject. Comparing the amplitudes of three consecutive waveforms gives two binary codes [a_1 a_2] denoting increase (i.e., 1) or decrease (i.e., 0). Similarly, [r_2 r_3] are binary codes representing increase or decrease in RRI of three successive cardiac cycles with a shift number of 1 (i.e., s = 1) shown on EKG.

Matching the two binary codes from changes in waveform amplitudes and the two binary codes of changes in RRI from EKG with left shift of one cardiac cycle gives a number 1 or 0.

$$\begin{aligned} [a_1 \ \ a_2] = [r_2 \ \ r_3] &\longrightarrow \text{count} + 1 \\ [a_1 \ \ a_2] \neq [r_2 \ \ r_3] &\longrightarrow \text{count} + 0 \end{aligned} \tag{15}$$

Similarly, the process continues till the amplitude of the n^{th} waveform.

$$\begin{aligned} [a_{n-1} \ \ a_n] = [r_n \ \ r_{n+1}] &\longrightarrow \text{count} + 1 \\ [a_{n-1} \ \ a_n] \neq [r_n \ \ r_{n+1}] &\longrightarrow \text{count} + 0 \end{aligned} \tag{16}$$

Summation of all the numbers of matches (i.e., percussion number) is thus obtained and divided by the total number of vectors of pattern gives the "percussion rate" (14). For instance, if the number of impact points (m) is 2 with a delay of one cardiac cycle [i.e., shift number (s) = 1] (Figure 1), then

$$P_{s=1}^{m=2} = \frac{1}{n-2} \sum_{i=1}^{n-2} \text{count}(i). \tag{17}$$

Step 6. Because diabetes is known to delay the reaction time of baroreflex due to impaired sensitivity [2, 11, 17], we assume that there would be a delay in cardiac cycle from one to sn. Taking logarithm of the sum of percussion rates (P_s^m) from shift number 1 to sn (i.e., s = 1, 2, ..., sn) gives

$$\varphi^m(n) = \ln\left(\sum_{s=1}^{sn} P_s^m\right), \tag{18}$$

ln: natural logarithmic operation.

For the present study, $\varphi^{m=2}(n)$ was used to assess baroreflex sensitivity.

Step 7. Increase impact points (i.e., the embedded dimension) to (m+1) and repeat Steps 2–6 to get

$$P_s^{m+1} = \frac{1}{(n-m-s+2)} \sum_{i=1}^{n-m-s+2} \text{count}(i), \tag{19}$$

$$\varphi^{m+1}(n) = \ln\left(\sum_{s=1}^{sn} P_s^{m+1}\right). \tag{20}$$

In the current study, $\varphi^{m=3}(n)$ indicated the complexity of a biological system. The higher the value of $\varphi^{m=3}(n)$, the lower the complexity of the biological system.

Step 8. Therefore, percussion entropy index (PEI) can be defined from (18) and (20):

$$PEI(m, s, n) = \varphi^m(n) - \varphi^{m+1}(n), \tag{21}$$

$$= \ln\left[\frac{\sum_{s=1}^{sn} P_s^m}{\sum_{s=1}^{sn} P_s^{m+1}}\right]. \tag{22}$$

In (21) and (22), m represents the chosen impact points (i.e., vector dimension), s represents a shift number for B_{RRI}, and n is the data length.

In other words, the degree of similarity between the changes in the binary series of digital volume pulse (DVP) waveform amplitudes (B_{Amp}) and the corresponding fluctuations in the binary series of RRI (B_{RRI}) on electrocardiogram over n cardiac cycles were first compared using a vector dimension of m, taking into account the possible delay in baroreflex from one cardiac cycle to sn cardiac cycles. The computation was then repeated with a vector dimension of m+1 over the same set of data points. Subtraction of the latter from the former gave the percussion entropy index (PEI) as in (21). The present study adopted an embedded vector dimension number of 2 (i.e., impact points, m = 2) to compute the value of percussion entropy, $\varphi^{m=2}(n)$.

Similarly, using m = 3, the percussion entropy value, $\varphi^{m=3}(n)$, was obtained. PEI was then obtained through subtracting $\varphi^{m=3}(n)$ from $\varphi^{m=2}(n)$. Physiologically, $\varphi^{m=2}(n)$ represents baroreflex sensitivity, while $\varphi^{m=3}(n)$ reflects the complexity of a biological system. The higher the former, the more sensitive the baroreflex. By contrast, an elevated value of the latter denotes decreased complexity of the acquired signals that implicates an impaired physiological status. Therefore, the optimal physiological condition would be $\varphi^{m=2}(n) \gg \varphi^{m=3}(n)$ (i.e., a high PEI value) when both baroreflex sensitivity and physiological complexity are high.

2.4. Statistical Analysis. Average values are expressed as mean ± SD. One sample Kolmogorov-Smirnov test was used for testing the normality of distribution, while the Statistical Package for the Social Science (SPSS, version 14.0 for Windows, SPSS Inc. Chicago, II) was adopted for verifying the homoscedasticity of variables. The significance of difference in anthropometric, hemodynamic, and computational parameters (i.e., PEI, MEI_{SS}, LHR, SSR) among different groups was determined using independent sample *t*-test with Bonferroni correction. The correlation between parameters and risk factors for different groups was compared using Pearson correlation test with Bonferroni correction. For significant parameters acquired through univariate analysis, multivariate regression analysis was used for further verification of the statistical significance. SPSS was used for all statistical analyses.

In statistical hypothesis testing, the probability value (i.e., *p*-value) or asymptotic significance is the probability for a given statistical model that, when the null hypothesis is true, the statistical summary (e.g., the sample mean difference between two compared groups) would be greater than or equal to the actual observed results. Although the level of significance is commonly set to 0.05, the *p*-values may need to be corrected for multiple test comparison. For the purpose of the present study, a corrected *p*-value of 0.017 was used because of comparison among three groups (i.e., 0.05 divided by three). Pearson's correlation coefficient, also referred to as Pearson's r, is a measure of the linear correlation between two variables *X* and *Y*. It has a value between +1 and −1. While 1 stands for total positive linear correlation, 0 means no linear correlation, and −1 signifies total negative linear correlation.

3. Results

3.1. Choice of Shift Number for Percussion Entropy Index Computation. The changes in percussion entropy index with shift number in all testing subjects are shown in Figure 3. Successful discrimination among the three groups was noted at shift number 5. Therefore, shift number 5 was used for percussion entropy index computation to ensure adequate coverage of possible delays due to impaired baroreflex sensitivity; the parameters of this study were set at m = 2, n = 1000, and s = 1 to 5.

3.2. Comparison of Computational Parameters for Autonomic Function Assessment. The results of comparing the two

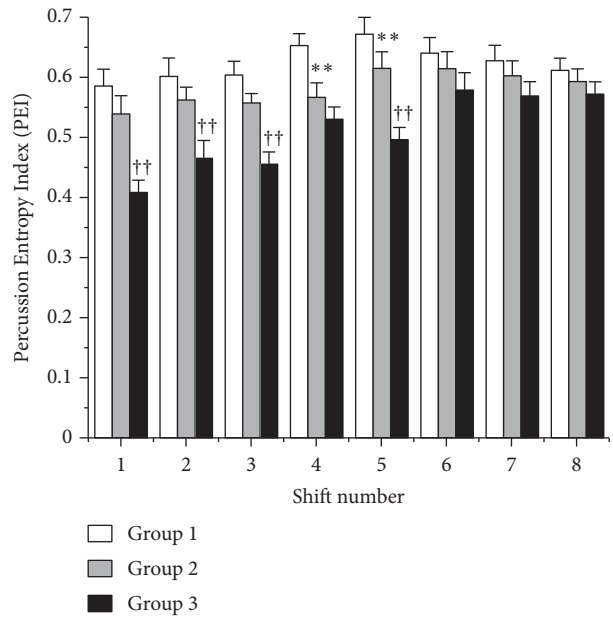

Figure 3: Changes in percussion entropy index of the three groups of testing subjects from shift number (s) of 1 to 8; $^{**}p < 0.001$: Group 1 vs. Group 2; $^{\dagger\dagger}p < 0.001$: Group 2 vs. Group 3; Group 1: healthy subjects; Group 2: diabetic subjects with satisfactory blood sugar control; Group 3: diabetic subjects with poor blood sugar control. Values are expressed as mean ± SD.

one-dimensional HRV-based computational parameters (i.e., LHR and SSR) with percussion entropy index (PEI) for autonomic function assessment among the three groups of testing subjects are shown in Table 2. Although SSR was significantly higher in Group 2 than that in Group 1 ($p < 0.017$), there was no notable difference in LHR among the three groups. On the other hand, both MEI_{SS} and PEI successfully discriminated among the three groups (all $p < 0.017$), although the discrimination between Group 1 and Group 2 was more significant with PEI ($p < 0.001$) compared to that with MEI_{SS} ($p < 0.017$).

3.3. Correlations of Demographic, Anthropometric, Hemodynamic, and Serum Biochemical Data with Computational Parameters for Autonomic Function Assessment in All Testing Subjects. Significant associations were noted between LHR and serum triglyceride concentration as well as between SSR and fasting blood sugar concentration (both $p < 0.017$) (Table 3). MEI_{SS} showed a significant positive association with glycated hemoglobin level ($p < 0.005$), which is an index of chronic diabetes control, but not with fasting blood sugar concentration, an indicator of acute diabetes control. On the other hand, percussion entropy was significantly related to fasting blood sugar concentration ($p < 0.017$) and highly significantly associated with glycated hemoglobin level ($p < 0.001$).

3.4. Multivariate Analysis for PEI, MEI_{SS}, SSR, and LHR. The demographic, anthropometric, hemodynamic, and serum biochemical parameters of the testing subjects found to be

Table 2: Comparison of computational parameters for autonomic function assessment in three groups of testing subjects.

Parameters	Group 1 (n = 41)	Group 2 (n = 36)	Group 3 (n =31)
LHR	1.62 ± 1.03	1.59 ± 1.54	2.48 ± 2.43
SSR	0.47 ± 0.22	0.61 ± 0.27*	0.61 ± 0.31
MEI_{SS}	0.56 ± 0.08	0.54 ± 0.02*	0.44 ± 0.13††
PEI	0.73 ± 0.04	0.63 ± 0.05**	0.56 ± 0.06††

Group 1: healthy subjects; Group 2: diabetic subjects with satisfactory blood sugar control; Group 3: diabetic subjects with poor blood sugar control. Values are expressed as mean ± SD. LHR: low- to high-frequency power ratio; SSR: Poincaré index (SD1/SD2 ratio); MEI_{SS}: small-scale multiscale entropy index (mean value of sample entropy from time scale from 1 to 5); PEI: percussion entropy index; *$p < 0.017$: Group 1 vs. Group 2; **$p < 0.001$: Group 1 vs. Group 2; ††$p < 0.001$ Group 2 vs. Group 3.

Table 3: Associations of demographic, anthropometric, hemodynamic, and serum biochemical data with computational parameters for autonomic function assessment in all testing subjects.

	PEI		MEI_{SS}		SSR		LHR	
	r	*p*	*r*	*p*	*r*	*p*	*r*	*p*
Age (years)	0.10	0.562	0.06	0.662	0.02	0.832	0.09	0.398
BH (cm)	0.14	0.251	0.13	0.351	-0.02	0.887	0.17	0.142
BW (kg)	-0.10	0.397	-0.12	0.417	-0.07	0.580	0.14	0.244
WC (cm)	0.55	0.241	0.65	0.351	0.05	0.861	0.20	0.074
BMI (kg/m^2)	-0.16	0.173	0.03	0.573	-0.04	0.742	0.07	0.543
SBP (mmHg)	-0.06	0.641	-0.01	0.741	0.10	0.421	-0.02	0.870
DBP (mmHg)	0.06	0.620	0.07	0.650	0.10	0.409	0.10	0.419
PP (mmHg)	-0.15	0.189	-0.10	0.428	0.06	0.632	-0.10	0.436
HDL (mg/dL)	0.01	0.942	0.05	0.963	-0.01	0.946	-0.08	0.548
LDL (mg/dL)	-0.01	0.934	-0.06	0.534	-0.04	0.749	-0.10	0.449
Cholesterol (mg/dL)	-0.10	0.439	-0.09	0.539	-0.01	0.920	0.02	0.899
Triglyceride (mg/dL)	-0.09	0.468	-0.10	0.439	0.21	0.079	0.30	*0.012*
HbA1c (%)	0.16	*0.001*	0.14	*0.005*	0.11	0.371	0.01	0.946
FBS (mg/dL)	0.13	*0.012*	0.13	0.018	0.03	*0.014*	0.07	0.587

BH: body height; BW: body weight; WC: waist circumference; BMI: body mass index, SBP: systolic blood pressure; DBP: diastolic blood pressure; PP: pulse pressure; HbA1c: glycated hemoglobin; HDL: high-density lipoprotein cholesterol; LDL low-density lipoprotein cholesterol; FBS: fasting blood sugar. LHR: low- to high-frequency power ratio; SSR: Poincaré index (SD1/SD2 ratio); MEI_{SS}: small-scale multiscale entropy index (mean value of sample entropy from time scale from 1 to 5); PEI: percussion entropy index; $|r| \leqq 0.3$: correlation of low significance; $0.3 \leqq |r| \leqq 0.7$: correlation of moderate significance; $0.7 \leqq |r| \leqq 1$: highly significant correlation. *$p < 0.017$; **$p < 0.001$. Significance of correlations determined with Pearson correlation.

Table 4: Multivariate linear regression analysis for percussion entropy index (PEI), LHR, and SSR for all subjects (n = 108).

	PEI			MEI_{SS}			SSR			LHR		
	B-Coef	β	*p*	B-Coef	β	*p*	B-Coef	β	*p*	B-Coef	β	*p*
Variable												
FBS (mg/dL)	0.824	0.123	0.012	0.825	0.053	0.032	0.841	0.096	0.022	0.826	0.042	0.853
HbA1c (%)	0.654	0.714	<0.001	0.702	0.156	<0.001	0.734	0.037	0.041	0.724	0.129	0.566
Constant	0.894	-	<0.001	0.507	-	0.003	1.750	-	0.010	0.409	-	0.008

B-Coef: regression coefficient; β: standardized coefficient; FBS: fasting blood sugar; HbA1c: glycated hemoglobin; PEI: percussion entropy index; MEI_{SS}: small-scale multiscale entropy index (mean value of sample entropy from time scale from 1 to 5); SSR: Poincaré index (SD1/SD2 ratio); LHR: low- to high-frequency power ratio.

significantly associated with PEI in this study using Pearson correlation test were fasting blood sugar concentration and glycated hemoglobin level for which multivariate analysis was performed (Table 4). The results showed significant associations of PEI with fasting blood sugar and glycated hemoglobin levels in all subjects as a whole without focusing on the effects of age and diabetes (all $p < 0.05$). In addition, the interpreting effects [37] of the two independent variables, glycated hemoglobin level and fasting blood sugar concentration, on dependent variable PEI were 71.4% and 12.3%, respectively. In other words, with multiple linear regression, the results of the present study demonstrated an 83.7% accuracy when the two independent variables (i.e., glycated hemoglobin level and fasting blood sugar

concentration) were used to describe the dependent variable (i.e., PEI). In contrast, the interpreting effects of glycated hemoglobin level and fasting blood sugar concentration (i.e., independent variables) on the dependent variable MEI_{SS} were comparatively low at 15.6% and 5.3%, respectively.

4. Discussion

Diabetes is a common metabolic disease characterized by vasculopathy commonly involving the eyes [6] and kidneys [7]. Neuropathy is another well-known diabetes-associated complication [8]. Using the method of multiscale cross-approximate entropy, we previously investigated the feasibility of adopting a multiscale cross-approximate entropy index in detecting diabetes-related arterial stiffness as reflected by the crest time (CT) of the study subjects [38]. The results of that study indicated that although multiscale cross-approximate entropy could identify diabetes-associated subtle changes in vascular functional integrity, it failed to demonstrate the impact of diabetes on autonomic nervous function [38]. Therefore, focusing on diabetes-associated autonomic neuropathy, the present study proposed a new approach to the assessment of baroreflex impairment through comparing the tendency of changes between the primary time series (i.e., Amp that reflects fluctuations in blood pressure) and the secondary time series (i.e., RRI that indicates corresponding baroreflex-triggered heart rate alterations) among three successive cardiac cycles. Meanwhile, taking into account the healthy physiological complexity of human body, lack of variation in the tendency of changes among four successive cardiac cycles is regarded as unhealthy and was used as a negative contributor to computation of the percussion entropy index. The results of the current study indicated that, through taking into account the physiology of baroreflex [14–16], this novel approach could give additional information on diabetic autonomic dysfunction through comparing the pattern of changes between two simultaneously acquired physiological time series (i.e., digital volume pulse amplitude and R-R interval).

The present study, which attempted to assess the impact of diabetes and its control on autonomic nervous function by comparing the tendency of changes of two simultaneous physiological time series (i.e., DVP amplitude and RRI) in subjects with and without the disease, has several interesting implications. First, among the three one-dimensional approaches to HRV analysis [i.e., frequency (i.e., LHR) and time (i.e., SSR) domain as well as multiscale (i.e., MEI_{SS})], only MEI_{SS} successfully discriminated among nondiabetic subjects as well as those with diabetes with and without satisfactory blood sugar control. Besides, the two-dimensional percussion entropy index (PEI) showed better ability to differentiate between healthy subjects and those with well-controlled diabetes than that of MEI_{SS}. Second, PEI was the only parameter with significant correlations with both acute (i.e., fasting blood sugar concentration) and chronic (i.e., glycated hemoglobin level) blood sugar control indicators. Third, strong interpreting effects from the two independent sugar control variables were noted only for PEI but not MEI_{SS}, LHR, and SSR. The results, therefore, highlight its notable sensitivity in detecting diabetes-associated autonomic dysfunction.

Previous studies have demonstrated that diabetes is associated with suppressed autonomic activities and blunted baroreflex [19, 39]. Previous studies have demonstrated the use of frequency domain [17–19] and time domain [20, 23] parameters in noninvasively assessing autonomic nervous function in diabetic patients but their sensitivities remain unclear. Taking into account the fact that baroreflex sensitivity is an indicator of autonomic function [15] as well as previous findings showing a good correlation between DVP signals and real-time changes in blood pressure [26–28], the current study investigated the possibility of assessing autonomic sensitivity through quantifying the matches between the two time series of DVP and RRI with a shift number of 1 to 5 based on the finding of a previous report that showed a delay of BRS between one to five heartbeats [16]. The finding of our study was consistent with that study [16] that using a shift number of 5 provided the best discriminating ability for PEI (Figure 3).

While considering the integrity of baroreflex by choosing a dimension of vector pattern (i.e., impact point, m) of 2, the physiological health of an individual as reflected in the complexity of signals was taken into account through adding a dimension of vector pattern of 3 into the computation of percussion entropy index (PEI). The major difference between multiscale entropy (MSE) and PEI is that the former evaluates changes in actual sample values within a defined range over time, whereas the latter simply compares the pattern of fluctuation between two related time series. In addition to utilizing the concept of MSE, PEI also encompasses the assessment of baroreflex sensitivity (BRS) (i.e., m = 2; higher value in (8) stands for higher BRS) and complexity (i.e., m =3; higher value in (10) represents lower complexity).

The present study has its limitations. First, the number of testing subjects in each group was relatively small. Nevertheless, highly significant associations between percussion entropy and indices of blood sugar control were still noted. Second, direct assessment of baroreflex sensitivity with either invasive or noninvasive means was not performed for comparison with the results of the current study.

5. Conclusions

This study demonstrated the validity of gaining additional information on diabetic autonomic dysfunction through comparing two simultaneously acquired physiological time series (i.e., digital volume pulse amplitude and R-R interval). The significant associations of percussion entropy with the indices of blood sugar control also highlight its possible role in early screening of the disease. The successful identification of the markers for diabetes by comparing the nonlinear coupling behavior of two synchronized time series of different natures raises the possibility of identifying the risk factors for diseases of other organs through analyzing the complexity of synchronized physiological signals related to the respective organ systems.

Data Availability

No data were used to support this study.

Conflicts of Interest

The authors declare that there are no conflicts of interest regarding the publication of this paper.

Authors' Contributions

Hsien-Tsai Wu has equal contribution compared with the corresponding author.

Acknowledgments

This research was supported by the National Science Foundation of China under Grant No. 61861001, Natural Science Foundation of Ningxia (No. NZ17050). The authors also gratefully acknowledge financial support for this work by the Key Laboratory of Intelligent Perception Control in North Minzu University, Ningxia, advanced intelligent perception control technology innovation team, Ningxia first-class discipline and scientific research projects (electronic science and technology NXYLXK2017A07).

References

[1] World Health Organization, "Global report on diabetes," 2016.

[2] M. Debono and E. Cachia, "The impact of Cardiovascular Autonomic Neuropathy in diabetes: is it associated with left ventricular dysfunction?" *Autonomic Neuroscience: Basic and Clinical*, vol. 132, no. 1-2, pp. 1–7, 2007.

[3] P. O. Bonetti, L. O. Lerman, and A. Lerman, "Endothelial dysfunction: a marker of atherosclerotic risk," *Arteriosclerosis, Thrombosis, and Vascular Biology*, vol. 23, no. 2, pp. 168–175, 2003.

[4] F. Grover-Páez and A. B. Zavalza-Gómez, "Endothelial dysfunction and cardiovascular risk factors," *Diabetes Research and Clinical Practice*, vol. 84, no. 1, pp. 1–10, 2009.

[5] J. Pearson-Stuttard, B. Zhou, V. Kontis, J. Bentham, M. J. Gunter, and M. Ezzati, "Worldwide burden of cancer attributable to diabetes and high body-mass index: a comparative risk assessment," *The Lancet Diabetes & Endocrinology*, vol. 6, no. 6, pp. e6–e15, 2018.

[6] D. A. Antonetti, R. Klein, and T. W. Gardner, "Diabetic retinopathy," *The New England Journal of Medicine*, vol. 366, no. 13, pp. 1227–1239, 2012.

[7] G. Remuzzi, A. Schieppati, and P. Ruggenenti, "Clinical practice. Nephropathy in patients with type 2 diabetes," *The New England Journal of Medicine*, vol. 346, no. 15, pp. 1145–1151, 2002.

[8] A. I. Vinik, "Clinical practice. Diabetic sensory and motor neuropathy," *The New England Journal of Medicine*, vol. 374, no. 15, pp. 1455–1464, 2016.

[9] J.-P. Le Floch, J. Doucet, B. Bauduceau, and C. Verny, "Retinopathy, nephropathy, peripheral neuropathy and geriatric scale scores in elderly people with type 2 diabetes," *Diabetic Medicine*, vol. 31, no. 1, pp. 107–111, 2014.

[10] S. Lankhorst, S. W. M. Keet, C. S. E. Bulte, and C. Boer, "The impact of autonomic dysfunction on peri-operative cardiovascular complications," *Anaesthesia*, vol. 70, no. 3, pp. 336–343, 2015.

[11] J. D. Lefrandt, A. J. Smit, C. J. Zeebregts, R. O. Gans, and K. H. Hoogenberg, "Autonomic dysfunction in diabetes: a consequence of cardiovascular damage," *Current Diabetes Reviews*, vol. 6, no. 6, pp. 348–358, 2010.

[12] V. Spallone, D. Ziegler, R. Freeman et al., "Cardiovascular autonomic neuropathy in diabetes: clinical impact, assessment, diagnosis, and management," *Diabetes/Metabolism Research and Reviews*, vol. 27, no. 7, pp. 639–653, 2011.

[13] H. V. Huikuri, V. Jokinen, M. Syvänne et al., "Heart rate variability and progression of coronary atherosclerosis," *Arteriosclerosis, Thrombosis, and Vascular Biology*, vol. 19, no. 8, pp. 1979–1985, 1999.

[14] G. D. Pinna, M. T. La Rovere, R. Maestri, A. Mortara, J. T. Bigger, and P. J. Schwartz, "Comparison between invasive and non-invasive measurements of baroreflex sensitivity: implications for studies on risk stratification after a myocardial infarction," *European Heart Journal*, vol. 21, no. 18, pp. 1522–1529, 2000.

[15] N. Wada, W. Singer, T. L. Gehrking, D. M. Sletten, J. D. Schmelzer, and P. A. Low, "Comparison of baroreflex sensitivity with a fall and rise in blood pressure induced by the valsalva manoeuvre," *Clinical Science (London)*, vol. 127, no. 5, pp. 307–313, 2014.

[16] P. Martínez-García, C. Lerma, and O. Infante, "Baroreflex sensitivity estimation by the sequence method with delayed signals," *Clinical Autonomic Research*, vol. 22, no. 6, pp. 289–297, 2012.

[17] R. Dalla Pozza, S. Bechtold, W. Bonfig et al., "Impaired short-term blood pressure regulation and autonomic dysbalance in children with type 1 diabetes mellitus," *Diabetologia*, vol. 50, no. 12, pp. 2417–2423, 2007.

[18] C. Li, Q. Chang, J. Zhang, and W. Chai, "Effects of slow breathing rate on heart rate variability and arterial baroreflex sensitivity in essential hypertension," *Medicine (Baltimore)*, vol. 97, no. 18, article e0639, 2018.

[19] M. Rosengård-Bärlund, L. Bernardi, J. Holmqvist et al., "Deep breathing improves blunted baroreflex sensitivity even after 30 years of type 1 diabetes," *Diabetologia*, vol. 54, no. 7, pp. 1862–1870, 2011.

[20] A. M. Climent, M. D. L. S. Guillem, D. Husser, F. Castells, J. Millet, and A. Bollmann, "Poincaré surface profiles of RR intervals: a novel noninvasive method for the evaluation of preferential AV nodal conduction during atrial fibrillation," *IEEE Transactions on Biomedical Engineering*, vol. 56, no. 2, pp. 433–442, 2009.

[21] V. Spallone and G. Menzinger, "Diagnosis of cardiovascular autonomic neuropathy in diabetes," *Diabetes*, vol. 46, no. 2, pp. S67–S76, 1997.

[22] G. Merati, M. Di Rienzo, G. Parati, A. Veicsteinas, and P. Castiglioni, "Assessment of the autonomic control of heart rate variability in healthy and spinal-cord injured subjects: contribution of different complexity-based estimators," *IEEE Transactions on Biomedical Engineering*, vol. 53, no. 1, pp. 43–52, 2006.

[23] C. Lerma, O. Infante, H. Pérez-Grovas, and M. V. José, "Poincare plot indexes of heart rate variability capture dynamic adaptations after haemodialysis in chronic renal failure patients," *Clinical Physiology and Functional Imaging*, vol. 23, no. 2, pp. 72–80, 2003.

[24] M. Costa, A. L. Goldberger, and C.-K. Peng, "Multiscale entropy analysis of complex physiologic time series," *Physical Review Letters*, vol. 89, no. 6, Article ID 068102, 2002.

[25] N. Takahashi, M. Nakagawa, T. Saikawa et al., "Noninvasive assessment of the cardiac baroreflex: Response to downward tilting and comparison with the phenylephrine method," *Journal of the American College of Cardiology*, vol. 34, no. 1, pp. 211–215, 1999.

[26] I. Jeong, S. Jun, D. Um, J. Oh, and H. Yoon, "Non-invasive estimation of systolic blood pressure and diastolic blood pressure using photoplethysmograph components," *Yonsei Medical Journal*, vol. 51, no. 3, pp. 345–353, 2010.

[27] H. Shin and S. D. Min, "Feasibility study for the non-invasive blood pressure estimation based on ppg morphology: normotensive subject study," *Biomedical Engineering Online*, vol. 16, no. 1, p. 10, 2017.

[28] X. Xing and M. Sun, "Optical blood pressure estimation with photoplethysmography and fft-based neural networks," *Biomedical Optics Express*, vol. 7, no. 8, pp. 3007–3020, 2016.

[29] American Diabetes Association, "Diagnosis and classification of diabetes mellitus," *Diabetes Care*, vol. 37, supplement 1, pp. S81–S90, 2014.

[30] H. T. Wu, P. C. Hsu, C. F. Lin et al., "Multiscale entropy analysis of pulse wave velocity for assessing atherosclerosis in the aged and diabetic," *IEEE Transactions on Biomedical Engineering*, vol. 58, no. 10, pp. 2978–2981, 2011.

[31] H. T. Wu, K. W. Lee, W. Y. Pan, A. B. Liu, and C. K. Sun, "Difference in bilateral digital volume pulse as a novel noninvasive approach to assessing arteriosclerosis in aged and diabetic subjects: a preliminary study," *Diabetes & Vascular Disease Research*, vol. 14, no. 3, pp. 254–257, 2017.

[32] P.-C. Hsu, H.-T. Wu, and C.-K. Sun, "Assessment of subtle changes in diabetes-associated arteriosclerosis using photoplethysmographic pulse wave from index finger," *Journal of Medical Systems*, vol. 42, no. 3, p. 43, 2018.

[33] A.-B. Liu, P.-C. Hsu, Z.-L. Chen, and H.-T. Wu, "Measuring pulse wave velocity using ECG and photoplethysmography," *Journal of Medical Systems*, vol. 35, no. 5, pp. 771–777, 2011.

[34] J. S. Richman and J. R. Moorman, "Physiological time-series analysis using approximate entropy and sample entropy," *American Journal of Physiology-Heart and Circulatory Physiology*, vol. 278, no. 6, pp. H2039–H2049, 2000.

[35] M. Costa, A. L. Goldberger, and C. K. Peng, "Multiscale entropy analysis of biological signals," *Physical Review E: Statistical, Nonlinear, and Soft Matter Physics*, vol. 71, no. 2, Article ID 021906, pp. 1–18, 2005.

[36] W.-Y. Pan, M.-C. Su, H.-T. Wu, T.-J. Su, M.-C. Lin, and C.-K. Sun, "Multiscale entropic assessment of autonomic dysfunction in patients with obstructive sleep apnea and therapeutic impact of continuous positive airway pressure treatment," *Sleep Medicine*, vol. 20, pp. 12–17, 2016.

[37] F. E. Harrell Jr., "Describing, resampling, validating, and simplifying the model," in *Regression Modeling Strategies with Applications to Linear Models, Logistic and Ordinal Regression, and Survival Analysis*, F. E. Harrell Jr., Ed., Springer Series in Statistics, pp. 103–126, Springer, Switzerland, 2015.

[38] M.-X. Xiao, H.-C. Wei, Y.-J. Xu, H.-T. Wu, and C.-K. Sun, "Combination of R-R interval and crest time in assessing complexity using multiscale cross-approximate entropy in normal and diabetic subjects," *Entropy*, vol. 20, no. 7, pp. 1–15, 2018.

[39] A. N. Syamsunder, P. Pal, G. K. Pal et al., "Decreased baroreflex sensitivity is linked to the atherogenic index, retrograde inflammation, and oxidative stress in subclinical hypothyroidism," *Endocrine Research*, vol. 42, no. 1, pp. 49–58, 2017.